MODELING AND CAPACITY OF REALISTIC SPATIAL MIMO CHANNELS

Akbar M. Sayeed

Department of Electrical and Computer Engineering
University of Wisconsin-Madison
1415 Engineering Drive, Madison, WI 53706
akbar@engr.wisc.edu, http://dune.ece.wisc.edu

ABSTRACT

Accurate and tractable channel modeling is critical to realizing the full potential of antenna arrays in wireless communications. In this paper we propose a framework for modeling multi-antenna multipath channels based on the notion of virtual spatial angles. The virtual angles are fixed a priori and are determined by the number of antennas at the transmitter and receiver and the spacing between the antennas. The model essentially corresponds to a coordinate transformation via fixed spatial basis functions at the transmitter and receiver. The resulting linear virtual channel representation encompasses all existing models and provides a natural link between the physical propagation environment and the channel statistics induced by it. For any given scattering environment, the model facilitates realistic estimates of channel capacity and clearly reveals the two key parameters affecting capacity: the number of parallel channels and the level of diversity.

1. INTRODUCTION

Antenna arrays holds great promise for bandwidth-efficient communication over the harsh wireless channel. Maximal exploitation of antenna arrays in wireless communication necessitates accurate yet computationally tractable modeling of the multi-input multi-output (MIMO) channel coupling the transmitter and receiver. Existing models represent two extreme approaches. On the one hand are *statistical* models that are idealized abstractions of spatial propagation characteristics and assume independent fading between different transmit-receive element pairs. These models have been heavily used in capacity calculations (see, e.g., [1]) and development of space-time coding techniques. On the other hand are *physical* models, inspired by array processing techniques, that explicitly model signal copies arriving from different directions. While more accurate descriptions of the actual propagation environment, these models are nonlinear in spatial angles, thereby making it rather difficult to incorporate them in transceiver design and capacity computations. Furthermore, the two approaches to MIMO antenna array modeling exist in virtual isolation. A connection relating them is very much desirable so that conclusions and insights derived from the two approaches can be cross-leveraged from improved transceiver designs.

There have been some recent attempts at bridging the gap between the two modeling philosophies (see, e.g., [2, 3]). However, these approaches are heavily entrenched in the physical modeling paradigm and suffer from the drawbacks associated with nonlinear modeling. We propose an approach that keeps the essence of physical modeling without its complexity and imposes a natural structure on channel statistics. Specifically, we model the channel with respect to fixed spatial basis functions defined by fixed virtual angles that are determined by the spatial array resolution. This is analogous to beamspace ideas in array processing and yields an analytically tractable linear channel characterization. The virtual channel matrix also provides an intuitively appealing "image" of the underlying scattering geometry that yields a simple interpretation of the two key factors affecting channel capacity: *the number of parallel of channels and the level of diversity*. The simple interpretation is formalized by a family of virtual channel models that capture the two factors and yield a simple formula for channel capacity. The virtual approach encompasses all existing modeling techniques and provide a natural framework for modeling and estimating the capacity of realistic scattering environments.

The next section introduces virtual modeling of multi-antenna channels and relates it to existing physical and statistical approaches. Section 3 discusses a family of virtual channel models for capturing realistic scattering environments. Section 4 illustrates capacity calculations via virtual channel models.

2. VIRTUAL CHANNEL MODELING

Consider a transmitter array with n_T elements and a receiver array with n_R elements. In the absence of noise, the transmitted and received signals are related as

$$\boldsymbol{x} = \boldsymbol{H}\boldsymbol{s} \tag{1}$$

where $\boldsymbol{s}$ is the n_T dimensional transmitted signal, $\boldsymbol{x}$ is the n_R dimensional received signal and $\boldsymbol{H}$ denotes the channel matrix coupling the transmitter and receiver elements. Most capacity calculations use this model and assume $\boldsymbol{H}$ to consist of independent, identically distributed (iid) Gaussian random variables — an idealized, rich scattering environment.

Explicit modeling of physical propagation effects can be used to impose structure on $\boldsymbol{H}$ as illustrated in Figure 1. The most widely used *physical* model is

$$\boldsymbol{H} = \sum_{l=1}^{L} \beta_l \boldsymbol{a}_R(\phi_{R,l})\boldsymbol{a}_T^H(\phi_{T,l}) = \boldsymbol{A}_R(\underline{\phi}_R)\boldsymbol{H}_P\boldsymbol{A}_T^H(\underline{\phi}_T) \tag{2}$$

which couples the transmitter and the receiver via L propagation paths with $\{\phi_{T,l}\}$ and $\{\phi_{R,l}\}$ as the spatial angles seen by the

This research was supported in part by the National Science Foundation under CAREER grant CCR-9875805 and grant ECS-9979408.

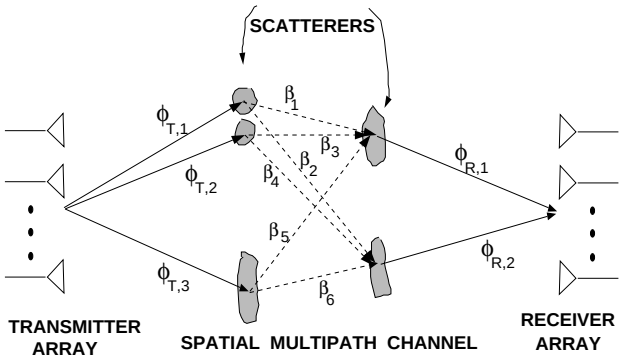

Fig. 1. *A schematic illustrating* **physical** *channel modeling. Each scattering path is associated with a fading gain (β_l) and a unique pair of transmit and receive angles ($\phi_{T,l}$, $\phi_{R,l}$) that connect physical scatterers distributed within the angular channel spreads.*

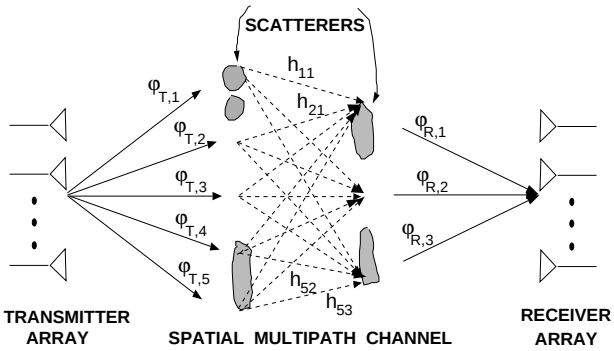

Fig. 2. *A schematic illustrating* **virtual** *channel modeling. The virtual angles are fixed a priori and their spacing is determined by the antenna spacing and defines the spatial resolution. Virtual channel representation does not distinguish between scatterers that are within the spatial resolution; the scatterers corresponding to the physical angles $\phi_{T,1}$ and $\phi_{T,2}$ in Figure 1, for example. The channel is characterized by the coefficients, $\{H_V(p,q) = h_{p,q}\}$, that couple the n_T virtual transmit angles, $\{\varphi_{T,p}\}$, with the n_R virtual receive angles, $\{\varphi_{R,q}\}$. For angles where there is no significant scattering, the corresponding coefficients are approximately zero (e.g., h_{21} and h_{52}).*

transmitter and receiver, respectively, and $\{\beta_l\}$ as the corresponding fading gains. The angles $\{\phi_{R,l}\}$ lie in within S_R, the angular spread of scatterers as seen by the receiver, whereas $\{\phi_{T,l}\}$ lie within S_T, the angular spread of scatterers as seen by the transmitter. $\boldsymbol{a}_R(\phi_R)$ represents the array response vector for a plane wave arriving from the direction ϕ_R and $\boldsymbol{a}_T(\phi_T)$ represents the transmitter steering vector for the direction ϕ_T. In the case of uniform linear arrays with spacings d_R and d_T at the transmitter and receiver, respectively, the array steering and response vectors take the form[1]

$$\boldsymbol{a}_T(\phi_T) = \left[1,\ e^{-j2\pi\theta_T}, \cdots, e^{-j2\pi(n_T-1)\theta_T}\right]^T \quad (3)$$

$$\boldsymbol{a}_R(\phi_R) = \left[1,\ e^{-j2\pi\theta_R}, \cdots, e^{-j2\pi(n_R-1)\theta_R}\right]^T \quad (4)$$

where $\theta_T = d_T \sin(\phi_T)/\lambda$ and $\theta_R = d_R \sin(\phi_R)/\lambda$. In the matrix representation in (2), $\boldsymbol{A}_R(\underline{\phi}_R) = [\boldsymbol{a}_R(\phi_{R,1}), \cdots, \boldsymbol{a}_R(\phi_{R,L})]$ is an $n_R \times L$ matrix, $\boldsymbol{A}_T(\underline{\phi}_T) = [\boldsymbol{a}_T(\phi_{T,1}), \cdots, \boldsymbol{a}_T(\phi_{T,L})]$ is an $n_T \times L$ matrix, and $\boldsymbol{H}_P = \text{diag}(\beta_1, \cdots, \beta_L)$ is an $L \times L$ diagonal matrix. The model is *linear* in the channel gains $\{\beta_l\}$ but *nonlinear* in the spatial angles $\{\phi_{R,l}, \phi_{T,l}\}$.

The finite dimensionality of the spatial signal space (due to the finite number of antenna elements) can be exploited to develop a *linear* channel model which uses spatial beams in *fixed, virtual* directions. The *virtual* model, illustrated in Figure 2, can be expressed as

$$\boldsymbol{H} = \sum_{q=1}^{n_R}\sum_{p=1}^{n_T} H_V(q,p)\boldsymbol{a}_R(\varphi_{R,q})\boldsymbol{a}_T^H(\varphi_{T,p}) = \widetilde{\boldsymbol{A}}_R \boldsymbol{H}_V \widetilde{\boldsymbol{A}}_T^H \quad (5)$$

where $\{\varphi_{R,q}\}$ and $\{\varphi_{T,p}\}$ are *fixed* virtual angles that result in full-rank matrices $\widetilde{\boldsymbol{A}}_R = [\boldsymbol{a}_R(\varphi_{R,1}), \cdots, \boldsymbol{a}_R(\varphi_{R,Q})]$ $(n_R \times n_R)$ and $\widetilde{\boldsymbol{A}}_T = [\boldsymbol{a}_T(\varphi_{T,1}), \cdots, \boldsymbol{a}_T(\varphi_{T,P})]$ $(n_T \times n_T)$. The $n_R \times n_T$ matrix $\boldsymbol{H}_V$ is the virtual channel representation. The following represent a natural choice for virtual spatial angles

$$\varphi_{T,p} = \sin^{-1}\left(\frac{p\lambda}{n_T d_T}\right) \quad , \quad \varphi_{R,q} = \sin^{-1}\left(\frac{q\lambda}{n_R d_R}\right) \quad (6)$$

where $p = -(n_T-1)/2, \cdots, (n_T-1)/2$ for n_T odd and $p = -n_T/2, \cdots, n_T/2-1$ for n_T even, and similarly for the index q in (6). For the above choice of angles, the matrices $\widetilde{\boldsymbol{A}}_R$ and $\widetilde{\boldsymbol{A}}_T$ are unitary — discrete Fourier transform matrices.

Virtual channel modeling is analogous to beamspace ideas used in array processing. The extent of the spatial horizon covered by the virtual angles depends on the spacing between the antenna elements. For $d_T = d_R = \lambda/2$, the virtual angles (6) cover the entire ($[-\pi/2, \pi/2]$) spatial horizon. However, larger antenna spacings result in a narrower antenna beam with spatially aliased copies of the beam spanning the entire spatial horizon. This is particularly useful in spatial multiplexing applications. In contrast to the physical model (2), the virtual model is *linear* and is characterized by $\boldsymbol{H}_V$. However, the matrix $\boldsymbol{H}_V$ is not diagonal in general.

Since $\widetilde{\boldsymbol{A}}_R$ and $\widetilde{\boldsymbol{A}}_T$ are unitary, $\boldsymbol{H}_V$ is related to $\boldsymbol{H}$ as

$$\boldsymbol{H}_V = \widetilde{\boldsymbol{A}}_R^H \boldsymbol{H} \widetilde{\boldsymbol{A}}_T \quad (7)$$

and thus $\boldsymbol{H}_V$ is *unitarily equivalent* to $\boldsymbol{H}$ and captures all information. In fact, $\boldsymbol{H}_V$ can be thought of as a Fourier domain representation of $\boldsymbol{H}$. Similarly, $\boldsymbol{H}_V$ is related to $\boldsymbol{H}_P$ as

$$\boldsymbol{H}_V = \widehat{\boldsymbol{A}}_R(\underline{\phi}_R)\boldsymbol{H}_P\widehat{\boldsymbol{A}}_T^H(\underline{\phi}_T) \quad (8)$$

where $\widehat{\boldsymbol{A}}_R(\underline{\phi}_R) = \widetilde{\boldsymbol{A}}_R^H \boldsymbol{A}_R(\underline{\phi}_R) = [\widehat{\boldsymbol{a}}_R(\phi_{R,1}), \cdots, \widehat{\boldsymbol{a}}_R(\phi_{R,L})]$ is a $n_R \times L$ matrix whose columns represent the projection of the physical array response vectors onto the virtual array response vectors and $\widehat{\boldsymbol{A}}_T(\underline{\phi}_T) = \widetilde{\boldsymbol{A}}_T^H \boldsymbol{A}_T(\underline{\phi}_T) = [\widehat{\boldsymbol{a}}_T(\phi_{T,1}), \cdots, \widehat{\boldsymbol{a}}_T(\phi_{T,L})]$ is a similarly defined $n_T \times L$ matrix. We note that the vector $\widehat{\boldsymbol{a}}(\phi_l)$ (at the transmitter or receiver) peaks at the few virtual angles in the neighborhood of the physical angle ϕ_l.

3. VIRTUAL MODELING OF REALISTIC CHANNELS

Realistic scattering environments can be modeled via a superposition of scattering clusters with limited angular spreads (see, e.g., [2]). By imposing a structure on the non-vanishing elements of

[1] Formulations for arbitrary geometries can also be developed.

$\boldsymbol{H}_V$, we can capture a fairly rich class of realistic scattering environments with a corresponding statistical model for $\boldsymbol{H}$. Each cluster corresponds to a nonvanishing submatrix of $\boldsymbol{H}_V$ and can be construed as a separate spatial channel . Virtual modeling clearly reveals the two key factors that affect the capacity of each cluster: 1) the number of virtual angles within the angular spread which determine the rank of the matrix and hence the number of parallel channels, and 2) the nature of scattering within the cluster which determines the level of diversity.

Realistic virtual channel modeling is motivated by the "image" of the physical scattering geometry provided by $\boldsymbol{H}_V$, as illustrated in Figure 3 for two clusters. Consider a single cluster of dense contiguous scatterers with $S_R = [S_{R-}, S_{R+}] \subset [-\pi/2, \pi/2]$ and $S_T = [S_{T-}, S_{T+}] \subset [-\pi/2, \pi/2]$. The nonvanishing submatrix of $H_V(p,q)$ for this cluster corresponds to $q = Q_-, \cdots, Q_+$, $p = P_-, \cdots, P_+$ where $Q_- \approx \lfloor n_R \sin(S_{R-}) d_R/\lambda \rfloor$, $Q_+ \approx \lceil n_R \sin(S_{R+}) d_R/\lambda \rceil$, and similarly for P_- and P_+. Thus, the rank r of $\boldsymbol{H}$ in this case is given by $r \approx \min(Q_+ - Q_- + 1, P_+ - P_- + 1)$. For example, for the top left cluster in Figure 3, $S_R = [\pi/16, 3\pi/16]$ and $S_T = [-3\pi/16, -\pi/16]$. For $n_T = n_R = 21$ and $d_T = d_R = \lambda/2$, this yields $(Q_-, Q_+) = (2, 6)$ and $(P_-, P_+) = (-2, -6)$ resulting in a 5×5 cluster submatrix. $\boldsymbol{H}_V$ corresponding to multiple clusters is a superposition of nonvanishing cluster submatrices, as in Figure 3. The rank of $\boldsymbol{H}$ is bounded by the sum of the ranks of cluster submatrices of $\boldsymbol{H}_V$.

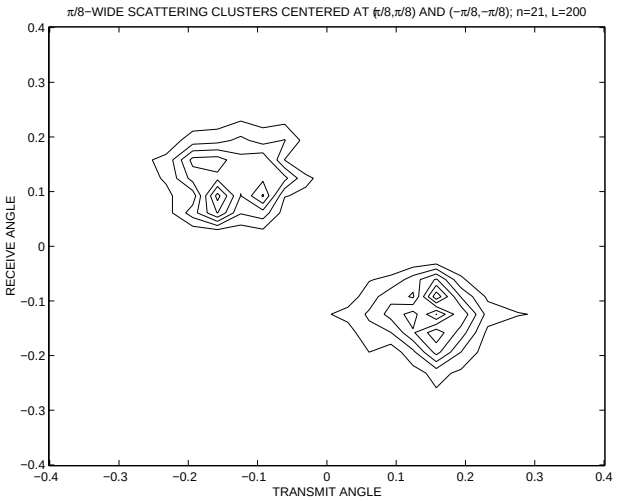

Fig. 3. *"Imaging" of the scattering environment via $\boldsymbol{H}_V$. $n_T = n_R = 21$ and $\boldsymbol{H}$ is generated via the physical model (2) using $L = 200$ paths associated with two $\pi/8$-wide clusters centered at $(\phi_T, \phi_R) = (\pi/8, -\pi/8)$ and $(-\pi/8, \pi/8)$.*

The nature of scattering within each cluster determines the diversity afforded by each cluster. To illustrate this concept, let $n_T = n_R = n$ and consider a single cluster covering the entire spatial horizon ($S_{R-} = S_{T-} = -\pi/2$ and $S_{R+} = S_{T+} = \pi/2$). On one extreme is "diagonal scattering" ($\boldsymbol{H}_V$ diagonal) in which each transmit virtual angle couples only with a single virtual receive angle. On the other extreme "maximally rich" scattering in which each transmit virtual angle couples with all virtual receive angles (all elements of $\boldsymbol{H}_V$ nonzero). This suggests the following k-diagonal virtual model to capture the nature of scattering in the two extreme and intermediate cases

$$\boldsymbol{H}_k = \sum_{p=1}^{n} \sum_{q=\max(1,p-k)}^{\min(n,p+k)} H_V(q,p) \boldsymbol{a}_R(\varphi_{R,q}) \boldsymbol{a}_T^H(\varphi_{T,p}) \qquad (9)$$

where $0 \le k \le n-1$. $k = 0$ corresponds to diagonal scattering and $k = n-1$ corresponds to maximally rich scattering.

We note that the elements of $\boldsymbol{H}_V$ are always approximately uncorrelated under the assumption of uncorrelated spatial scattering (uncorrelated β_l in (2)) Using this fact, the above k-diagonal model directly imposes a structure on the statistics of $\boldsymbol{H}$. Let $\boldsymbol{h}_k = \text{vec}(\boldsymbol{H}_k)$ where $\text{vec}(\boldsymbol{H})$ represents a vector obtained by stacking the columns of $\boldsymbol{H}$. The correlation matrix $\boldsymbol{R}_k = \text{E}[\boldsymbol{h}_k \boldsymbol{h}_k^H]$ takes the form

$$\begin{aligned} \boldsymbol{R}_k \quad = \quad & \sum_{p=1}^{n} \sum_{q=\max(1,p-k)}^{\min(n,p+k)} \sigma_{q,p}^2 [\boldsymbol{a}_T(\varphi_{T,p}) \otimes \boldsymbol{a}_R(\varphi_{R,q})] \\ & [\boldsymbol{a}_T^H(\varphi_{T,p}) \otimes \boldsymbol{a}_R^H(\varphi_{R,q})] \end{aligned} \qquad (10)$$

where $\otimes$ represents the kronecker product and we have used the identity $\text{vec}(\boldsymbol{ADB}) = [\boldsymbol{B}^H \otimes \boldsymbol{A}]\text{vec}(\boldsymbol{D})$. In (10), $\sigma_{q,p}^2 = \text{E}[|H_V(q,p)|^2]$ is the power in each uncorrelated virtual channel coefficient. The nonzero $\{\sigma_{q,p}^2\}$ in (10) represent active scattering between the p^{th} transmit q^{th} receive virtual angles. We note that $k = n-1$ and $\sigma_{q,p}^2 = 1$ in (10) corresponds to maximally rich scattering and yields the extreme case of iid elements of $\boldsymbol{H}$ ($\boldsymbol{R}_n = \boldsymbol{I}$) that is assumed in most capacity calculations. For diagonal virtual scattering ($k = 0$ in (10)), there is significant correlation between elements of $\boldsymbol{H}$. As demonstrated in the next section, $\boldsymbol{H}_0$ (diagonal) and $\boldsymbol{H}_{n-1}$ (iid) have nearly identical ergodic capacities (same rank) under appropriate power normalization, but radically different outage capacities due to higher diversity in $\boldsymbol{H}_{n-1}$.

4. VIRTUAL CAPACITY CALCULATIONS

In this section, we illustrate the ease of computation and simple interpretation afforded by virtual modeling for capacity calculations. We first discuss two key parameters that control capacity and relate them to physical characteristics. Our focus here is on outage capacity, a metric more appropriate in fading channels. The capacity of a fading channel is a random variable under decoding delay constraints and outage capacity reflects the maximum rate that can be guaranteed with a certain probability.

Parallel Channels and Diversity: The "image" of the scattering environment provided by $\boldsymbol{H}_V$ is intimately related to two key parameters that affect channel capacity: the number of *parallel channels*, P, that controls ergodic capacity, and the level of *diversity per parallel channel*, D, that controls the outage capacity. $P \le P_{max} = \min(n_T, n_R)$ and there have to be at least $L = \min(n_T, n_R)$ physical paths with distinct transmit/receive virtual angles to achieve P_{max}. $D \le D_{max} = \max(n_T, n_R)$ and in order to achieve D_{max} each virtual transmit angle must couple with D_{max} distinct virtual receive angles via different paths. Thus, we need at least $\min(n_T, n_R) \times \max(n_T, n_R) = n_T \times n_R$ physical paths corresponding to distinct virtual angles to achieve both $P = P_{max}$ and $D = D_{max}$. This requires maximum scattering spreads and maximally rich scattering. Smaller spreads and less rich scattering results in lower values of P and D. For example, the diagonal model $\boldsymbol{H}_0$ can achieve $P = P_{max}$ but $D = 1$

whereas the full iid model $\boldsymbol{H}_{n-1}$, can attain both $P = P_{max}$ and $D = D_{max}$. We note that the requirement for paths with distinct virtual angles is important — for example, if all paths are confined within the virtual spatial resolution, P and D will be close to 1 no matter how many paths there are.

Capacity Expressions: Consider the noisy channel, $\boldsymbol{x} = \sqrt{P}\boldsymbol{H}\boldsymbol{s} + \boldsymbol{w}$, where P is the transmitted power ($\mathrm{E}[\|\boldsymbol{s}\|^2] = 1$) and $\boldsymbol{w}$ is zero-mean complex Gaussian noise vector with $\mathrm{E}[\boldsymbol{w}\boldsymbol{w}^H] = \boldsymbol{I}$. Given the knowledge of channel coefficients ($\boldsymbol{H}$ or $\boldsymbol{H}_V$) at the receiver, the channel capacity is given by [1]

$$C(\boldsymbol{H}_V) = \log_2 \left[\det\left(\boldsymbol{I} + P\boldsymbol{H}_V\boldsymbol{H}_V^H/n\right)\right] \quad bits/s/Hz \quad (11)$$

where we have used unitary equivalence of $\boldsymbol{H}$ and $\boldsymbol{H}_V$. The ergodic capacity is given by $C_E = \mathrm{E}[C(\boldsymbol{H}_V)]$ where the expectation is over the statistics of $\boldsymbol{H}_V$. If the propagation environment consists of a superposition of scattering clusters, the imaging interpretation of $\boldsymbol{H}_V$ implies that (11) can be further simplified to

$$C(\boldsymbol{H}_V) = \sum_{i=1}^{N_c} \log_2 \left[\det(\boldsymbol{I} + P\boldsymbol{H}_V(i)\boldsymbol{H}_V^H(i)/n)\right] \quad bits/s/Hz \quad (12)$$

where N_c is the number of distinct clusters and $\boldsymbol{H}_V(i)$ is the submatrix corresponding to the i^{th} cluster.[2] For example, the two $\pi/8$-wide clusters in Figure 3, result in a block diagonal matrix $\boldsymbol{H}_V = \mathrm{diag}(\boldsymbol{H}_V(1), \boldsymbol{H}_V(2))$ consisting of two 5×5 matrices. Each $\boldsymbol{H}_V(i)$ in (12) can be further modeled as a k-diagonal virtual matrix representing the nature of scattering within the cluster. The cluster decomposition in (12) has the following simple approximate interpretation:

An arbitrary spatial channel can be decomposed into N_c independent parallel virtual channels that are represented by the matrices $\{\boldsymbol{H}_V(i) : i = 1, \cdots, N_c\}$, each $\boldsymbol{H}_V(i)$ in turn modeled by a k-diagonal iid matrix that reflects the nature of scattering in the cluster.

Numerical Examples: We present numerical results for two different environments: An idealized rich scattering environment and a more realistic environment consisting of two scattering clusters with smaller angular spreads. In both cases, $n_T = n_R = 10$ and SNR = $10\log_{10}(P)$ = 20dB.

The channel in the rich scattering case is directly modeled via $\boldsymbol{H}$ with elements given by iid complex zero-mean Gaussian random variables of unit variance. We compare the outage capacity of various k-diagonal virtual models computed from 1000 independent realizations of $\boldsymbol{H}$.[3] The matrix $\boldsymbol{H}_k$ is scaled so that the received SNR is the same as in all cases. Figure 4(a) illustrates this comparison which captures the effect of diversity on outage capacity — D increases with the number of diagonals k. As evident, the performance of a 3-diagonal approximation is very close to the iid channel ($k = 9$), demonstrating that for the same received SNR the 3-diagonal system captures most of the diversity advantage. We note that the ergodic capacity is virtually identical for all k.

Figure 4(b) compares the capacity of a more realistic scattering environment for different k-diagonal virtual approximations with no SNR normalization. $\boldsymbol{H}$ is simulated via the physical model (2) corresponding to two $\pi/8$-wide clusters centered at $\phi_R = \phi_T = \pm\pi/4$, analogous to Figure 3. There are $L = 100$ paths in each cluster. The angles $\{\phi_{T,l}, \phi_{R,l}\}$ for the paths are uniformly distributed over the angular spreads and the fading gains $\{\beta_l\}$ are simulated as iid zero-mean complex Gaussian random variables of unit variance. As evident, the capacity of a 2-diagonal virtual approximation is very close to that of the full iid (9-diagonal) channel. This is because D is relatively small in this case due to limited scattering spread.

[2]The relation (12) assumes that each cluster corresponds to distinct transmit and receive virtual angles. However, this assumption can be relaxed via a permutation of virtual angles.

[3]$\boldsymbol{H}_V$ for computing $\boldsymbol{H}_k$ in (9) is computed from $\boldsymbol{H}$ via (7)

5. REFERENCES

[1] G. J. Foschini, "Layered space-time architecture for wireless communication in a fading environment when using multi-element antennas," *Bell Labs Tech. J.*, vol. 1, no. 2, 1996.

[2] J. Fuhl, A. F. Molisch, and E. Bonek, "Unified channel model for mobile radio systems with smart antennas," in *IEE Proc. Radar, Sonar Navig.*, vol. 145, pp. 32–41, Feb. 1998.

[3] G. G. Raleigh and J. M. Cioffi, "Spatio-temporal coding for wireless communication," *IEEE Trans. Commun.*, Mar. 1998.

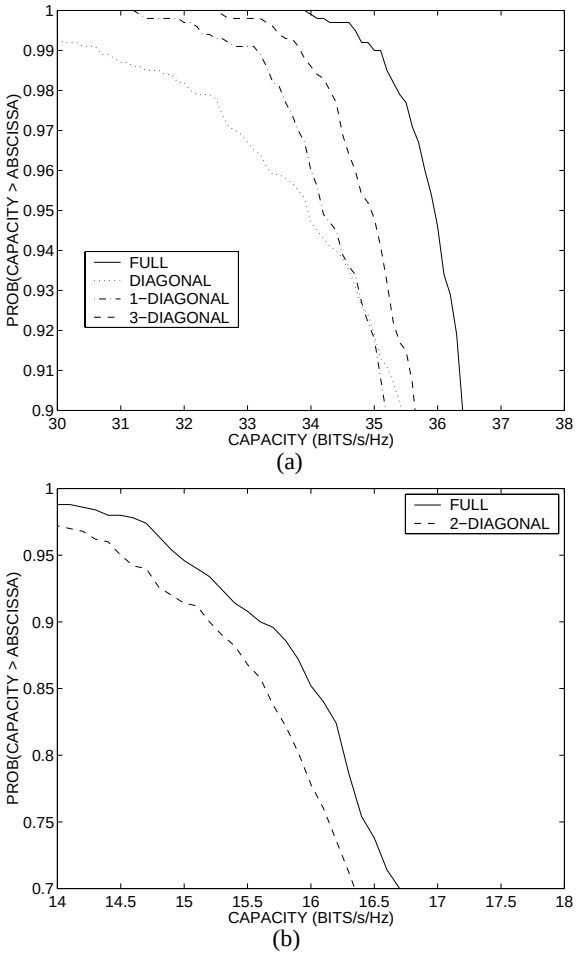

Fig. 4. *(a) Capacity comparison of k-diagonal models in a rich scattering environment with all models having the same received SNR. The level of diversity is the main difference between the models. (b) Capacity comparison without SNR normalization in a realistic environment consisting of two $\pi/8$-wide clusters.*